Diffusion in Phase Space as a Tool to Assess Variability of Vertical Centre-of-Mass Motion during Long-Range Walking

Nicolas Boulanger [1], Fabien Buisseret [2,3,4,*], Victor Dehouck [1,5], Frédéric Dierick [2,6,7] and Olivier White [5]

1 Physique de l'Univers, Champs et Gravitation, Université de Mons—UMONS, 20 Place du Parc, 7000 Mons, Belgium

2 CeREF, Chaussée de Binche 159, 7000 Mons, Belgium

3 Forme and Fonctionnement Humain Lab, Department of Physical Therapy, Haute Ecole Louvain en Hainaut, Rue Trieu Kaisin 136, 6061 Montignies sur Sambre, Belgium

4 Service de Physique Nucléaire et Subnucléaire, UMONS Research Institute for Complex Systems, Université Mons, 20 Place du Parc, 7000 Mons, Belgium

5 INSERM-U1093 Cognition, Action, and Sensorimotor Plasticity, Université de Bourgogne, Campus Universitaire, BP 27877, 21078 Dijon, France

6 Laboratoire d'Analyse du Mouvement et de la Posture (LAMP), Centre National de Réécation Fonctionnelle et de Réadaptation—Rehazenter, Rue André Vésale 1, 2674 Luxembourg, Luxembourg

7 Faculté des Sciences de la Motricité, Univercité Catholique Louvain (UCLouvain), Place Pierre de Coubertin 1-2, 1348 Ottignies-Louvain-la-Neuve, Belgium

* Correspondence: fabien.buisseret@umons.ac.be

Abstract: When a Hamiltonian system undergoes a stochastic, time-dependent anharmonic perturbation, the values of its adiabatic invariants as a function of time follow a distribution whose shape obeys a Fokker–Planck equation. The effective dynamics of the body's centre-of-mass during human walking is expected to represent such a stochastically perturbed dynamical system. By studying, in phase space, the vertical motion of the body's centre-of-mass of 25 healthy participants walking for 10 min at spontaneous speed, we show that the distribution of the adiabatic invariant is compatible with the solution of a Fokker–Planck equation with a constant diffusion coefficient. The latter distribution appears to be a promising new tool for studying the long-range kinematic variability of walking.

Keywords: gait variability; adiabatic invariant; random noise; Fokker-Planck equation; phase-space dynamics

1. Introduction

Action-angle coordinates $(I_\alpha, \theta^\alpha)$, with $\alpha = 1, \ldots, n$, are of central importance in the study of deterministic classical systems with finitely many degrees of freedom. A time-independent integrable Hamiltonian can indeed be formulated as a separable function of the action variables only: $H = \sum_{i=\alpha}^{n} H_{0\alpha}(I_\alpha)$. The equations of motion for such a system read ([1], Chapter 45):

$$\dot{I}_\alpha = -\frac{\partial H}{\partial \theta^\alpha} = 0, \quad \dot{\theta}^\alpha = \frac{\partial H}{\partial I_\alpha} =: \omega_\alpha . \tag{1}$$

The action variables are constants of the motion and therefore ω_α is also constant, implying that the angle coordinates read $\theta^\alpha = \omega_\alpha t + \theta_0^\alpha$, where $\omega_\alpha = 2\pi/T_\alpha$ and T_α is the period of the motion in the plane $(I_\alpha, \theta^\alpha)$. Since the Kolmogorov–Arnold–Moser theorem (see Refs. [2] (Ref. [3] for English translation), [4,5], and, for a historical overview, Ref. [6]) and the studies of Nekhoroshev [7,8], the action-angle variables have proven to be the most useful for the study of stability of dynamical systems, including chaotic systems. We now restrict our formalism to systems with $n = 1$, whose sole degrees of freedom consist in the pair (I, θ).

Suppose that H depends on a function $\lambda(t)$. The action variable I then becomes time-dependent and is called an adiabatic invariant. On the one hand, if λ changes slowly during the typical period of a cycle, then the adiabatic invariant also changes slowly: $\dot{I} \sim \dot{\lambda}$ [1,9,10]. On the other hand, if λ is a perturbative stochastic noise, the adiabatic invariant also becomes randomly time-dependent and the deviation from its average value remains perturbative. Detailed demonstrations and bounds for the deviation can be found in Refs. [11,12]. Moreover, for a Hamiltonian $H(I, \lambda(t))$ with perturbative stochastic noise $\lambda(t)$, it has been shown that the density $\rho(I, t)$ of the values of the adiabatic invariant as a function of time obeys a Fokker–Planck equation [13–15]. The latter phenomenon is a diffusion process in phase space. Besides its intrinsic interest, such a formalism has already found an important application in plasma physics, where it allows us to relax the standard simplifying assumptions and describe the problem in a less model-dependent way [16]. The Fokker–Planck equation has also been recently applied to the study of robustness in gene expression [17].

Biomechanical models of voluntary rhythmic movements in humans, of which walking has been studied most extensively, may also benefit from the above results. Such movements are quasi-periodic because of physiological noise, which prevents an individual from being in the same invariant state during repeated movements. The resulting variability has motivated many studies of human gait, most of which rely on the computation of nonlinear indices to assess variability (Hurst exponent, fractal dimension, etc.). See Refs. [18,19] for the pioneering studies and Refs. [20,21] for recent reviews. To our knowledge, the variability of gait has never been studied by assessing the shape and time evolution of the distribution $\rho(I, t)$. In the present paper, we show that the distribution, $\rho(I, t)$, in human walking indeed obeys a Fokker–Planck equation, i.e., that diffusion in phase space is experimentally observable in walking. Biomechanical models can then inherit the advantages of this formalism.

The paper is structured as follows. In Section 2, diffusion in phase space and its use in modelling human walking is proposed. Then, in Section 3, the experimental setup is presented and numerical results are given in Section 4. Finally, in Section 5, the results are discussed and concluding remarks are given.

2. Diffusion in Phase Space

2.1. Generalities

Let us consider a one-dimensional Hamiltonian, $H_0(I)$, where I and θ are the action and angle coordinates, respectively. Suppose that a time-dependent stochastic perturbation is added to H_0 and that the latter Hamiltonian satisfies the stability assumptions underlying the Nekhoroshev theorem [7,8]. The total Hamiltonian H can be written as follows:

$$H = H_0(I) + \epsilon \, \xi(t) \, \mathcal{V}(I, \theta) \, , \qquad (2)$$

where $0 < \epsilon \ll 1$ and $\xi(t)$ is a stochastic noise with a vanishing mean value. Under the dynamics controlled by H, the action variable becomes time-dependent and the deviation from the initial value I_0 is of order $\sqrt{\epsilon}$ up to a time of order $1/\epsilon$ or even better [11,12]. More precisely, $|I(t) - I_0| = O(\sqrt{\epsilon})$ and a time-dependent density distribution $\rho(I, t)$ of the values of the adiabatic invariant can be associated with its time evolution $I(t)$. As shown and illustrated in Refs. [13–15], the density distribution $\rho(I, t)$ obeys a particular Fokker–Planck equation given by

$$\partial_t \rho = \partial_I(D(I)\partial_I \rho) \, , \qquad (3)$$

where the function $D(I)$ is called the diffusion function and $\partial_I \equiv \partial/\partial_I$. Considering the Fourier decomposition, $\mathcal{V}(I, \theta) = \sum_k \mathcal{V}_k(I)\, e^{ik\theta}$, of the perturbation function that appears in the Hamiltonian, the following expression is obtained [15] for the diffusion function:

$$D(I) = \frac{\epsilon^2}{2} \sum_k k^2 |\mathcal{V}_k(I)|^2 \tilde{\phi}(k\omega) , \qquad (4)$$

where $\tilde{\phi}(\nu)$ is the noise spectral density, i.e., $\tilde{\phi}(\nu) = \int_{-\infty}^{+\infty} \phi(u) \cos(\nu u)\, du$ with the autocorrelation function,

$$\phi(u) = \lim_{T \to +\infty} \frac{1}{T} \int_0^T \xi(t)\xi(t+u)\, du . \qquad (5)$$

Two particular cases can be highlighted. First, when $H = (\omega + \epsilon\,\xi(t))I$, only the $k = 0$ mode $\mathcal{V}_0$ is non-zero and $D = 0$. There is no diffusion in a pure harmonic oscillator with a randomly perturbed frequency [13]. Second, in the case of a constant diffusion coefficient, the normalised solution of Equation (3) on the interval $I \in [0, +\infty)$ with boundary conditions, $\rho(I, 0) = \delta(I - I_0)\,\Theta(t)$, Θ being the Heaviside step function, $\delta(I - I_0)$ the Dirac delta function, and $\rho(0, t) = 0 = \lim_{I \to +\infty} \rho(I, t)$, can be obtained:

$$\rho(I, t) = \Theta(t)\, \frac{e^{-\frac{(I-I_0)^2}{4Dt}} - e^{-\frac{(I+I_0)^2}{4Dt}}}{\sqrt{4\pi Dt}\, \mathrm{erf}\left(\frac{I_0}{\sqrt{4Dt}}\right)} = \Theta(t)\, \frac{e^{-\frac{(I-I_0)^2}{4Dt}}}{\sqrt{4\pi Dt}}\, \frac{1 - e^{-\frac{I I_0}{Dt}}}{\mathrm{erf}\left(\frac{I_0}{\sqrt{4Dt}}\right)} . \qquad (6)$$

The normalisation is such that $\int_0^{+\infty} \rho(I, t)\, dI = \Theta(t)$. Hereafter, we are interested in the second case of a constant, but a non-vanishing diffusion function.

For a general discussion about the construction of solutions of the Fokker–Planck equation, see Ref. [22], and Refs. [23,24] for explicit solutions with non-constant and non-zero diffusion and drift coefficients.

2.2. Application to Human Walking

It is known that the vertical displacement of the body's centre-of-mass (COM) during human bipedal walking at spontaneous speed is compatible with a simple, spring-mass-like, model; see, for example, the seminal paper [25]. It is therefore tempting to model the vertical motion of the COM by the harmonic oscillator Hamiltonian, $H_0 = \frac{1}{2}(P^2 + \omega^2 Q^2) = \omega\, I$, where P and Q are the vertical momentum and position of the COM, respectively. By definition, and assuming the standard relation, $P \propto \dot{Q}$, one has

$$I = \frac{1}{2\pi} \oint_\Gamma P\, dQ = \frac{T \overline{E_c}}{\pi} , \qquad (7)$$

with Γ a cycle in phase space, T the duration of the cycle and $\overline{E_c}$ the averaged kinetic energy over Γ.

Some phenomena suggest that the inclusion of other terms, at least in the perturbation, is necessary to obtain a more realistic model. First, the minimum (maximum) of the potential energy and the maximum (minimum) of kinetic energy are not reached at exactly the same time: a time shift of about 3% of the gait cycle duration is observed [26]. Such a feature requires a time-dependent correction to be added. Second, the Hamiltonian H_0 corresponds to a linearised pendulum only in the limiting case of small amplitudes. Anharmonic corrections should be added. See Ref. [27] for a more explicit model of the pendulum, in which the potential term is nonlinear, and Ref. [28] for a computation of action-angle variables for the fully non-linear pendulum with Hamiltonian, $H_0 = P^2/2 + 1 - \cos Q$. Third, the parameters of the model (ω here) must have some time-dependent variability due to physiological noise; the state of a complex system like the human body is not identical from one gait cycle to another.

In view of the above discussion, a Hamiltonian of the form (2), in which H_0 contains anharmonic terms also, seems to be a relevant model of the vertical COM dynamics in

action-angle formalism. As far as the perturbation, $H_1(I, \theta) = \epsilon\, \xi(t)\, \mathcal{V}(I, \theta)$ is concerned, assuming a constant but non-vanishing diffusion coefficient, D, will considerably simplify the model. Referring to Equation (4), this implies that all functions, $\mathcal{V}_k(I)$, are constant, so that $H_1(I, \theta)$ only depends on the angle variable θ. H_1 does not depend on the total amount of action or energy in the system, but only on time through the stochastic noise, $\xi(t)$, and on the position in the cycle through $\mathcal{V}(\theta)$. Therefore, here, we assume that the influence of physiological noise on walking is related to the position in the gait cycle and not to the total action or the averaged kinetic energy of the walker—recall that $I \sim \overline{E_c}$. Consequently, Equation (3) with a non-zero diffusion coefficient yields the heat equation,

$$\partial_t \rho = D\, \partial_I^2 \rho \,, \tag{8}$$

and the diffusion of the adiabatic invariant should be observable experimentally.

3. Experimental Setup

3.1. Protocol

The protocol was validated by the Academic Ethical Committee Brussels Alliance for Research and Higher Education (B200-2021-123). Participants were healthy students recruited in the physiotherapy department of the Haute-Ecole Louvain en Hainaut (Montignies-sur-Sambre, Belgium). After being informed about the study, each participant signed an informed consent form.

Biometric data were first collected (age, weight, height), as well as information on the wearing of orthopaedic insoles and the participant's medical and trauma history. The participant is then asked to put on a tight-fitting garment. In order for his or her movements to be recorded by a Vicon optoelectronic system (Vicon Motion Systems Ltd., Oxford Metrics, Oxford, UK) consisting of 8 cameras (Vero version 2.2) with a recording frequency of 120 Hz, 4 reflective markers with a diameter of 14 mm were placed on the participant according the Plug-In-Gait model (Oxford Metrics, Oxford, UK): Left Anterior Superior Iliac Spine (LASI), Right Anterior Superior Iliac Spine (RASI), Left Posterior Superior Iliac Spine (LPSI), and Left Posterior Superior Iliac Spine (RPSI).

After this preparatory phase, the participant walked for 3 min on an N-Mill instrumented treadmill (Motekforce Link, Amsterdam, The Netherlands). The purpose of this familiarisation phase is to determine the participant's spontaneous walking speed. No other data were recorded during this period. After the walking speed was recorded, the participant walked on the treadmill for 10 min at the previously determined spontaneous speed. During these 10 min, the average number of steps per minute was measured by the treadmill and the three-dimensional trajectory of the 4 markers, $\vec{x}_a(t)$, was recorded by the Vicon system using the Vicon Nexus software (version 2.7.1, Oxford Metrics, Oxford, UK).

The general characteristics of the participants are listed in Table 1. Let us note that an initial analysis of these data was presented in a recent paper [29], in which we showed that an adiabatic invariant exists in the vertical motion of the COM. Here, we go further in the analysis to assess whether or not the variability of the latter adiabatic invariant is modelled by Equation (8).

Table 1. Features of the population. Results are written under the form median [Q1–Q3], with Q1 and $Q3$ being the first and third quartiles, respectively.

Population Feature	Median, Interval
Participants (n)	25
Age (years)	23 [20–23]
Mass (kg)	65.0 [58.8–73.4]
Height (cm)	169 [164–176]
Walking speed (km/h)	3.9 [3.5–4.2]
Sex (men/women)	9/16
Gait cycles	532 [513–552]

3.2. Data Processing

For a given participant, the position of the centre-of-mass is defined as the average position of the four markers: 6 $\vec{x}_{COM} = \sum_\alpha \vec{x}_\alpha / 4$. A focus in the study here is on the vertical component of the COM motion, $Q(t)$. To reduce measurement artefacts, $Q(t)$ was filtered with a fourth-order Butterworth low-pass filter, preserving 99.99% of the signal power. Cubic spline interpolation of the data was also performed, multiplying the frequency by 10 to 1200 Hz. The speed, $\dot{Q}$, is computed from the time series Q by finite differentiation.

An identification, $P = \dot{Q}$, is performed, i.e., standard Hamiltonian dynamics is assumed and the mass scale is set equal to 1 (this normalisation removes the variability induced by participants' masses). Then, we identify gait cycles by analysing the peaks in $Q(t)$: the duration of gait cycles i, $T_i = t_{i+2} - t_i$, were computed from the times t_i, at which the peaks occur. The times, t_i, can be defined as the times, atwhich a new step begin, a gait cycle consisting in two steps (left and right). Then, the average kinetic energies, $\overline{E_{ci}}$, were computed as the mean values of $\dot{Q}^2/2$ on the successive cycles, and the adiabatic invariants,

$$I_i = \frac{T_i \overline{E_{ci}}}{\pi} \tag{9}$$

were also computed.

The values collected in the sets $A_i = \{I_{j \leq i}\}$ are then binned according to Sturges rule [30], leading to n bins. The centres $I_a^{(i)}$, and the frequencies, $\varphi_a^{(i)}$, i.e., the number of items in bin a divided by total number of items, are computed, with $a = 1, \ldots, n$. The experimentally computed distribution, $\rho^{\exp}(t_i, I)$, of the adiabatic invariant after a walking duration, t_i, is defined via $\rho^{\exp}(t_i, I) = \left(I_a^{(i)}, \varphi_a^{(i)} \right)$.

A fit of the form (6) is then performed on the sets $\rho^{\exp}(t_{i \geq 100}, I)$ using the least-squares method and the parameters I_{0i} and D_i are recorded. The latter parameters are the fitted values of I_0 and D at time t_i. No fit was made for the first 100 points. This threshold is arbitrary, but avoids situations where the distribution has too little structure for the adjustment to be relevant. Finally, we compute the average values, $I_0 = E(I_{0i})$ and $D = E(D_i)$, resulting in a distribution (6) called the model, $\rho^{\text{th}}(t, I)$.

The compatibility of the experimental distributions $\rho^{\exp}(t_{i \geq 100}, I)$ and the model predictions $\rho^{\text{th}}(t_i, I)$ is assessed by a Kolmogorov–Smirnov test with a significance level of 0.05. Let us note Π, the percentage of tests with the p-value, $p > 0.05$, i.e., the percentage of cases, in which the model is incompatible with the experimental data. One-sample t-tests were performed with null hypothesis of zero mean for I_0 and D.

All the computations were performed using the free software R (version 4.1.0) [31].

4. Results

The attractors of the centred vertical position and speed of the COM versus time are shown in Figure 1A,B, along with a typical phase space trajectory shown in Figure 1C. The attractor is computed as follows. After each step cycle is identified, an average cycle is computed. For this purpose, each step was normalised to a duration of 1 time unit (0–100%). Then, 1200 bins, one for each frame, were created and filled with the data of all steps of a given participant under a given condition. For each bin, the mean and standard deviation were computed. This yields the average cycle, which we refer to as the attractor, following Refs. [32,33]. The attractor can be interpreted as the basic motor pattern that a participant tries to achieve during each step cycle—without achieving it exactly due to intrinsic physiological noise.

From the attractor, one can see that the effective dynamics is not a pure harmonic oscillator, as it moves away from an elliptical shape in the first quadrant, as indicated by a straight arrow in Figure 1C. Note that here we use the trigonometric convention in order to split the plane into four quadrants, with the angle going from 0 to $\pi/2$ in the first quadrant, from $\pi/2$ to π in the second quadrant, etc. The deformation is systematic and present in all participants. Therefore, the model presented in Section 2 can be applied since the

diffusion coefficient can be non-zero. Here, each step cycle starts when the COM is at its higher position and its speed is null, i.e., when the subject is in midstance: one foot on the ground, the knee is extended and the other foot is in swing phase and crossing the stance leg. The direction of the trajectory of the COM in phase space is clockwise: from the fourth to first quadrant. In the fourth and third quadrants, the COM position decreases (downward movement) and the speed is negative. The attractor shape is elliptical as in a spring-mass model of the stance leg [27], inducing a harmonic motion. In the second and first quadrants, the COM position increases (upward movement) and its speed is now positive. In the fourth quadrant, the participant is in a single leg stance (SS) on one foot and this phase continues during the first part of the third quadrant. In the second part of the third quadrant, the participant is in a dual stance (DS), which begins when the COM speed is at its lowest value and ends when the COM postion is at its lowest value [34]. At the end of the second quadrant and the first one, the participant is in single leg stance on the other foot.
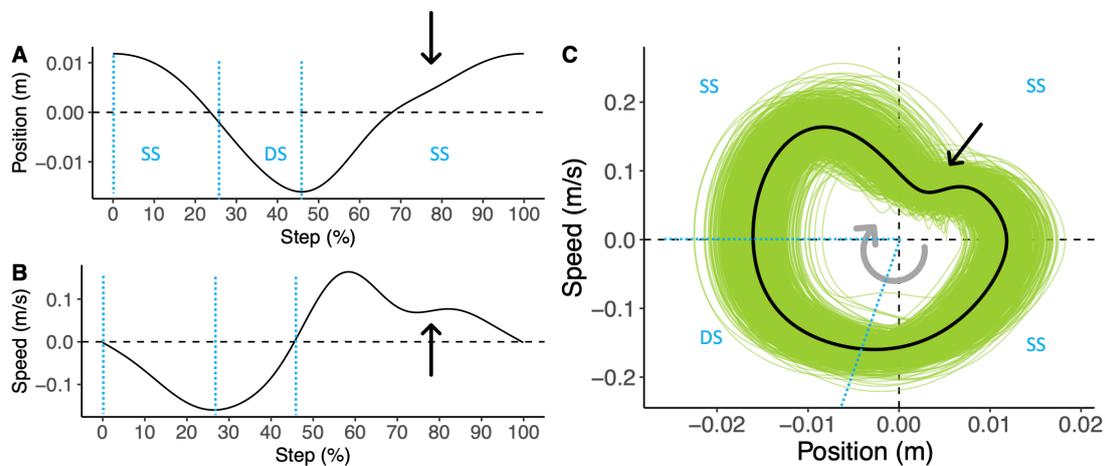

Figure 1. (**A**) Attractor of the centred vertical position of the body's centre-of-mass (COM) versus time, expressed in % of step time. (**B**) Attractor of the vertical speed of the COM versus time, expressed in % of step time. (**C**) Typical plot of COM vertical trajectory in phase space (solid green lines representing 508 gait cycles) during walking for a participant and of the corresponding attractor (solid black line). The straight arrows outline the deviation from genuine harmonic oscillator. The curved arrow is the arrow of time. Note that a closed loop corresponds to one step cycle, a complete gait cycle being composed of two step cycles. The blue dotted line separate the single stance (SS) and dual stance (DS) phases.

It appears that the fit is relevant since $\Pi > 97\%$ for 20 participants out of 25. Hence, the model (6) fairly well agrees with the time evolution of the distribution of the adiabatic invariant. Fitted parameters are summarized in Table 2. The mean value of I reads:

$$\langle I \rangle = \int_0^{+\infty} \rho(I,t)dI = \frac{\Theta(t)}{\mathrm{erf}\left(\frac{I_0}{\sqrt{4Dt}}\right)} I_0 \,, \tag{10}$$

and its behaviour versus time is displayed in Figure 2. The mean value stays of order I_0 during the protocol: Less than 10% of variation is observed. The values obtained are comparable to the mean value found by an independent analysis in Ref. [29]: $\pi \langle I \rangle = 0.0143 \pm 0.0058$ J·s/kg.

The ability of the model to fit the data can be appraised in Figure 3, where a typical plot of the fitted distributions versus experimental observations is displayed for one participant. All participants show the same qualitative agreement between the model and the data.
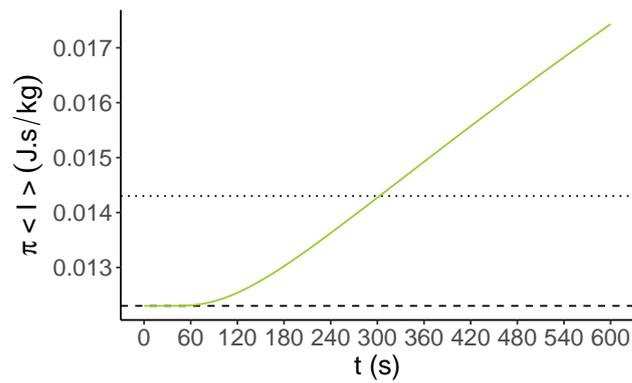
Figure 2. $\pi \langle I \rangle$ versus time (green line), see Equation (10). The median value given in Table 2 is indicated by the horizontal dashed line, while the average value found in Ref. [29] is shown by the dotted line.
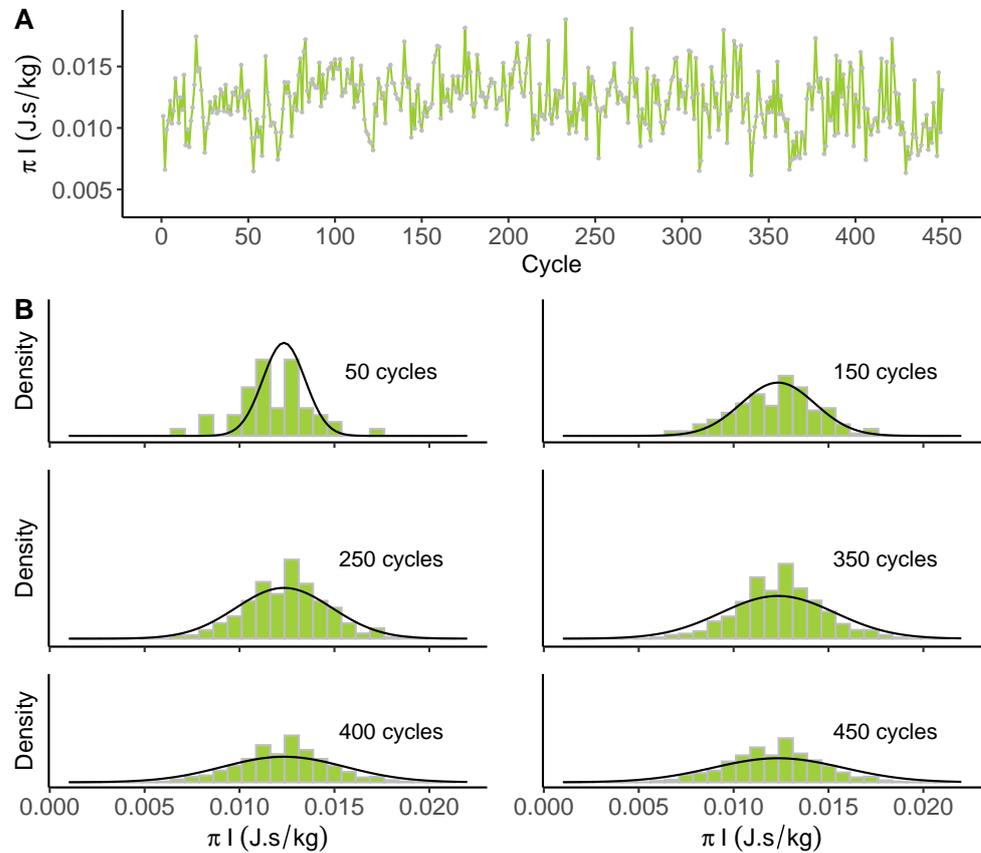

Figure 3. (**A**) Adiabatic invariant versus time (grey points) for a given participant. Lines are added to guide the eyes, and time is expressed in cycle number. (**B**) Typical plots showing the comparison between the theoretical distribution, $\rho^{\text{th}}(t_i, I)$ (solid line), and the experimental distribution, $\rho^{\text{exp}}(t_i, I)$ (histograms), after 50, 150, 250, 350, 400 and 450 cycles for the same participant as in (**A**), with $\Pi = 99.4\%$. Fitted parameters are equal to $\pi I_0 = 0.0123$ J·s/kg and $D = 1.05 \times 10^{-8}$ m^2/s. See text for details.

Table 2. Results of the fits of experimental distributions of the adiabatic invariants to model (6). Results are written under the form median [Q1–Q3]. The *p*-values of the one-sample *t*-tests are given.

Parameter	Fit Value	*p*-Value
D (10^{-9} m^2/s)	11.618 [6.024–37.712]	<0.001
πI_0 (J·s/kg)	0.0123 [0.0061–0.0178]	<0.001
Π (%)	100 [98.6–100]	

5. Discussion

By studying the vertical motion of the healthy participant during walking, in this paper, we show that the phenomenon of phase space diffusion can be observed through the distribution of adiabatic invariant values over time. To our knowledge, this is the first time that such an observation is made in human motion.

The time evolution of the distribution of the adiabatic invariant over time is compatible with the Fokker–Planck equation with a constant diffusion coefficient for healthy young adults walking at a spontaneous speed of progression. Thus, up to the experimental precision here, no drift and no deformation of the constant-D distribution for high or low values of I are observed. A change in the most likely value of I can presumably be associated with a change in energy expenditure during walking. As argued in Ref. [29], the value of the adiabatic invariant should be proportional to oxygen consumption during walking, and an increase in the former should be associated with an increase in the latter.

There are a number of immutable factors in the environment in which we live. One is gravity. The brain, instead of fighting against the effects caused by its presence (e.g., the emergence of a weight that counteracts movements) has developed strategies to make the most of it and optimize movements [35]. In other words, humans move more optimally in the presence than in the absence of a gravitational field. One can make a parallel with the existence of noise in physiological systems. These emerge at every level of the decision-action chain, from perception to motoneurons. The authors have proposed, in the optimal movement variability framework, that the central nervous system could actually exploit the presence of noise and, hence, act more optimally in the presence of certain levels of uncertainties. Following Refs. [36–38], we interpret the variability measured in this investigation by the distribution not as an "imperfection", but rather as an indication of the adaptability of the participants to the motor task. A given value of the adiabatic invariant corresponds to a given area in phase space for the step cycle under consideration. Thus, the changes in I indicate that the participants have access to a wide range of motor strategies, visualised as closed step cycles in phase space. The distribution becomes wider and wider over time: more and more different motor patterns are "explored". In the approach given in this paper, there is no drift: the most likely value of I, i.e., the attractor defined as the ideal trajectory in phase space that the participant is aiming for, does not change with time.

We conjecture that the shape of the distribution $\rho(I, t)$ might be sensitive to the experimental condition and/or to each participant, as shown in Figure 4. In particular, there should be an optimal values of the diffusion coefficient D and of I_0 for a young, healthy individual. Too large value obtained for D would reflect a lack of or altered motor control of the participant, leading to variability that tends to be random, as observed in the stride interval variability of patients with neurodegenerative diseases [39], for example. Too small value for D can be related to insufficient adaptability of the participant: the number of available patterns (i.e., different values of I) is not maximal. Such a case is observed, for example, in the electrocardiographic signal of patients with cardiovascular disease [36] or in healthy children, whose walking patterns are more stereotyped than in adults [40]. The diffusion coefficient then offers a novel way to quantify the general behaviour of internal models developed for a given task. Indeed, wide distributions (high D value) are observed after time spent to experience or explore a task. On the other hand, narrow distributions (small D value) may reflect a lack of generalisation of the motor strategies adopted. In motor control—and rehabilitation in particular—the concept of generalisation is tightly linked to the one of transfer [41–43]. When working toward recovering lost or impaired motor functions, the challenge is to find the best possible movements that can be transferred to as many functional tasks as possible. These movements may be interpreted as fundamental bricks of the action repertoire. An interesting question is why would a participant opt for a narrow distribution? One possible explanation for this is related to the way motor learning works. There are different learning mechanisms, the most powerful being error-based learning. In this one, one plans the best possible action by minimising a cost function

that includes target reaching in the general sense and effort. An error signal is observed in case of a discrepancy between observation and what has been predicted by forward models [44,45], which induces strategic changes, and encourages exploration. Another learning mechanism, however, co-exists with slower dynamics: use-dependent-learning. When relying on this mechanism, one tends to repeat the same action if it led to success in the past, thereby discouraging exploration in the task space. Adopting this strategy results from a compromise between cost and benefit: the target can be reached, but the control policy may be stuck in a local minima of the cost function.
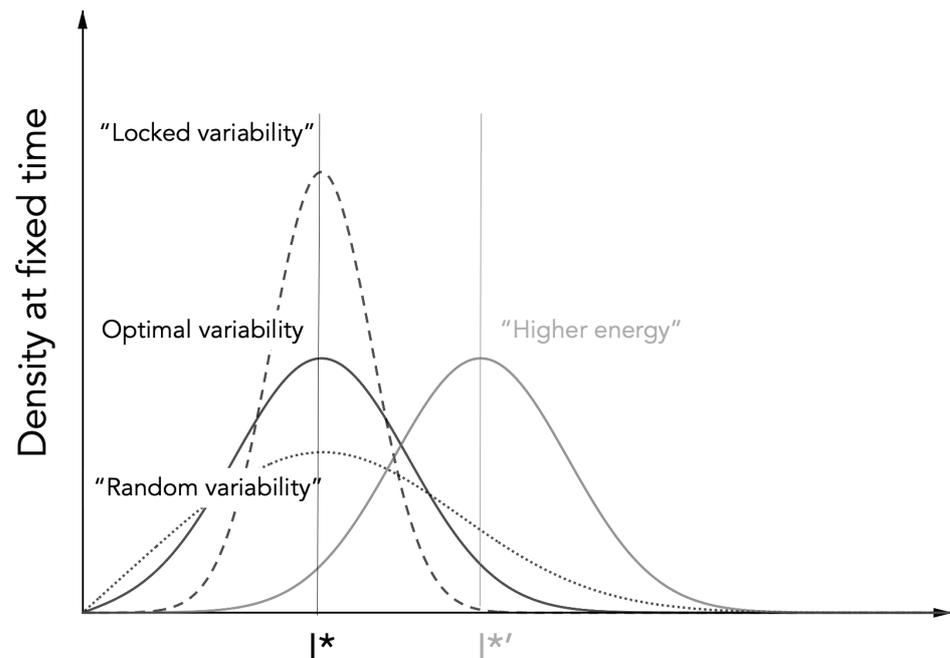
Figure 4. Schematic representation of several types of adiabatic invariant densities. Here is assumed that the black solid line is the density of a young, healthy, individual. The maximally probable adiabatic invariant in this case is denoted I^*. The "locked" (dashed line) and "random" (dotted line) curves correspond to, respectively, smaller and higher diffusion coefficients than the optimal one. The "higher energy" curve (grey solid line) has an optimal diffusion coefficient, but a higher maximally probable adiabatic invariant, denoted $I^{*\prime}$.

In the future, we consider to apply the present formalism to participants with different ages or experimental conditions to investigate the effects of deviations from the optimal "healthy young adult state" on $\rho(I, t)$. More precisely, our hope is to design appropriate experimental contexts that would manipulate I and D independently, then providing a better functional understanding of these indexes in motor control.

Author Contributions: Conceptualization, N.B. and F.B.; methodology, F.B. and V.D.; software, V.D. and F.B.; formal analysis, N.B. and F.B.; data curation, V.D.; writing—original draft preparation, N.B., F.B. and V.D.; writing—review and editing, N.B., F.B., F.D., O.W. and V.D. All authors have read and agreed to the published version of the manuscript.

Institutional Review Board Statement: The study was conducted according to the guidelines of the Declaration of Helsinki, and approved by the Academic Ethical Committee Brussels Alliance for Research, acceptance number: B200-2021-123.

Informed Consent Statement: Informed consent was obtained from all subjects involved in the study.

References

1. Landau, L.; Lifchitz, E. *Physique Théorique, Tome 1: Mécanique*; Éditions MIR: Moscow, Russia, 1988.
2. Kolmogorov, A.N. On conservation of conditionally periodic motions for a small change in Hamilton's function. *Dokl. Akad. Nauk SSSR* **1954**, *98*, 527–530. (In Russian)
3. Kolmogorov, A.N. Preservation of conditionally periodic movements with small change in the Hamilton function. In *Stochastic Behavior in Classical and Quantum Hamiltonian Systems*; Casati, G., Ford, J., Eds.; Springer: Berlin/Heidelberg, 1979; pp. 51–56. [CrossRef]
4. Arnol'd, V.I. Proof of a theorem of A.N. Kolmogorov on the invariance of quadi-periodic motions under small perturbations of the hamiltonian. *Russ. Math. Surv.* **1963**, *18*, 9–36. [CrossRef]
5. Möser, J. On invariant curves of area-preserving mappings of an annulus. *Nachr. Akad. Wiss. Göttingen II, Math.-Phys. Kl.* **1962**, *1962*, 1–20.
6. Scott Dumas, H. *The KAM Story: A Friendly Introduction to the Content, History, and Significance of Classical Kolmogorov-Arnold-Moser Theory*; World Scientific: Hackensack, NJ, USA, 2014. [CrossRef]
7. Nekhoroshev, N. Behavior of Hamiltonian systems close to integrable. *Funct. Anal. Its Appl.* **1971**, *5*, 338–339. [CrossRef]
8. Nekhoroshev, N. An exponential estimate of the time of stability of nearly-integrable Hamiltonian systems. *Russ. Math. Surv.* **1977**, *32*, 1–65. [CrossRef]
9. Henrard, J. The adiabatic invariant in classical mechanics. In *Dynamics Reported.*; Kirchgraber, U., Walther, H.O., Eds.; Springer: Berlin/Heidelberg, 1993; Volume 2, pp. 117–235. [CrossRef]
10. Jose, J.V.; Saletan, E.J. *Classical Dynamics: A Contemporary Approach*; Cambridge University Press: Cambridge, UK, 1998. [CrossRef]
11. Khas'minskii, R.Z. On Stochastic processes defined by differential equations with a small parameter. *Theory Probab. Its Appl.* **1966**, *11*, 211–228. [CrossRef]
12. Cogburn, R.; Ellison, J.A. A stochastic theory of adiabatic invariance. *Commun. Math. Phys.* **1992**, *149*, 97–126. [CrossRef]
13. Bazzani, A.; Siboni, S.; Turchetti, G.; Vaienti, S. A model of modulated diffusion. I. Analytical results. *J. Stat. Phys.* **1994**, *76*, 929–967. [CrossRef]
14. Bazzani, A.; Siboni, S.; Turchetti, G. Diffusion in stochastically and periodically modulated Hamiltonian systems. *AIP Conf. Proc.* **1995**, *344*, 68–77. [CrossRef]
15. Bazzani, A.; Beccaceci, L. Diffusion in Hamiltonian systems driven by harmonic noise. *J. Phys. A Math. Gen.* **1998**, *31*, 5843–5854. [CrossRef]
16. Kominis, Y.; Ram, A.K.; Hizanidis, K. Kinetic Theory for Distribution Functions of Wave-Particle Interactions in Plasmas. *Phys. Rev. Lett.* **2010**, *104*, 235001. [CrossRef]
17. Degond, P.; Herda, M.; Mirrahimi, S. A Fokker-Planck approach to the study of robustness in gene expression. *Math. Biosci. Eng.* **2020**, *17*, 6459–6486. [CrossRef]
18. Hausdorff, J.M.; Peng, C.K.; Ladin, Z.; Wei, J.Y.; Goldberger, A.L. Is walking a random walk? Evidence for long-range correlations in stride interval of human gait. *J. Appl. Physiol.* **1995**, *78*, 349–358. [CrossRef]
19. Hausdorff, J.M.; Mitchell, S.L.; Firtion, R.; Peng, C.K.; Cudkowicz, M.E.; Wei, J.Y.; Goldberger, A.L. Altered fractal dynamics of gait: Reduced stride-interval correlations with aging and Huntington's disease. *J. Appl. Physiol.* **1997**, *82*, 262–269. [CrossRef]
20. Stergiou, N.A. *Nonlinear Analysis for Human Movement Variability*; CRC Press/Taylor & Francis Group: Boca Raton, FL, USA, 2016; Volume 7. [CrossRef]
21. Ravi, D.K.; Marmelat, V.; Taylor, W.R.; Newell, K.M.; Stergiou, N.; Singh, N.B. Assessing the temporal organization of walking variability: A systematic review and consensus guidelines on detrended fluctuation analysis. *Front. Physiol.* **2020**, *11*, 562. [CrossRef]
22. Risken, H. *The Fokker-Planck Equation: Methods of Solution and Applications Second Edition*; Springer: Berlin/Heidelberg, Germany, 1996. [CrossRef]
23. Fa, K.S. Exact solution of the Fokker-Planck equation for a broad class of diffusion coefficients. *Phys. Rev. E* **2005**, *72*, 020101. [CrossRef]
24. Lin, W.T.; Ho, C.L. Similarity solutions of the Fokker–Planck equation with time-dependent coefficients. *Ann. Phys.* **2012**, *327*, 386–397. [CrossRef]

25. Cavagna, G.; Thys, H.; Zamboni, A. The sources of external work in level walking and running. *J. Physiol.* **1976**, *262*, 639–657. [CrossRef]

26. Cavagna, G.A.; Legramandi, M.A. The phase shift between potential and kinetic energy in human walking. *J. Exp. Biol.* **2020**, *223*, jeb232645. [CrossRef]

27. Whittington, B.R.; Thelen, D.G. A simple mass-spring model with roller feet can induce the ground reactions observed in human walking. *J. Biomech. Eng.* **2008**, *131*, 011013. [CrossRef]

28. Brizard, A.J. Jacobi zeta function and action-angle coordinates for the pendulum. *Commun. Nonlinear Sci. Numer. Simul.* **2013**, *18*, 511–518. [CrossRef]

29. Buisseret, F.; Dehouck, V.; Boulanger, N.; Henry, G.; Piccinin, F.; White, O.; Dierick, F. Adiabatic Invariant of Center-of-Mass Motion during Walking as a Dynamical Stability Constraint on Stride Interval Variability and Predictability. *Biology* **2022**, *11*, 1334. [CrossRef] [PubMed]

30. Sturges, H.A. The Choice of a Class Interval. *J. Am. Stat. Assoc.* **1926**, *21*, 65–66. [CrossRef]

31. The R Project for Statistical Computing. Available online: https://www.r-project.org (accessed on 10 January 2023).

32. Broscheid, K.-C.; Dettmers, C.; Vieten, M. Is the Limit-Cycle-Attractor an (almost) invariable characteristic in human walking? *Gait Posture* **2018**, *63*, 242–247. [CrossRef]

33. Raffalt, P.; Kent, J.; Wurdeman, S.; Stergiou, N. To walk or to run—A question of movement attractor stability. *J. Exp. Biol.* **2020**, *223*, jeb224113. [CrossRef]

34. Adamczyk, P.G.; Kuo, A.D. Redirection of center-of-mass velocity during the step-to-step transition of human walking. *J. Exp. Biol.* **2009**, *212*, 2668–2678. [CrossRef]

35. White, O.; Gaveau, J.; Bringoux, L.; Crevecoeur, F. The gravitational imprint on sensorimotor planning and control. *J. Neurophysiol.* **2020**, *124*, 4–19. [CrossRef]

36. Goldberger, A.L.; Amaral, L.A.N.; Hausdorff, J.M.; Ivanov, P.C.; Peng, C.K.; Stanley, H.E. Fractal dynamics in physiology: Alterations with disease and aging. *Proc. Natl. Acad. Sci. USA* **2002**, *99*, 2466–2472. [CrossRef] [PubMed]

37. Stergiou, N.; Harbourne, R.; Cavanaugh, J. Optimal movement variability: A new theoretical perspective for neurologic physical therapy. *J. Neurol. Phys. Ther.* **2006**, *30*, 120–129. [CrossRef]

38. van Emmerik, R.E.; Ducharme, S.W.; Amado, A.C.; Hamill, J. Comparing dynamical systems concepts and techniques for biomechanical analysis. *J. Sport Health Sci.* **2016**, *5*, 3–13. [CrossRef]

39. Moon, Y.; Sung, J.; An, R.; Hernandez, M.E.; Sosnoff, J.J. Gait variability in people with neurological disorders: A systematic review and meta-analysis. *Hum. Mov. Sci.* **2016**, *47*, 197–208. [CrossRef] [PubMed]

40. Hausdorff, J.M.; Zemany, L.; Peng, C.K.; Goldberger, A.L. Maturation of gait dynamics: Stride-to-stride variability and its temporal organization in children. *J. Appl. Physiol.* **1999**, *86*, 1040–1047. [CrossRef] [PubMed]

41. Dizio, P.; Lackner, J.R. Motor adaptation to Coriolis force perturbations of reaching movements: Endpoint but not trajectory adaptation transfers to the nonexposed arm. *J. Neurophysiol.* **1995**, *74*, 1787–1792. [CrossRef]

42. Criscimagna-Hemminger, S.E.; Donchin, O.; Gazzaniga, M.S.; Shadmehr, R. Learned dynamics of reaching movements generalize from dominant to nondominant arm. *J. Neurophysiol.* **2003**, *89*, 168–176. [CrossRef]

43. Sarwary, A.M.E.; Stegeman, D.F.; Selen, L.P.J.; Medendorp, W.P. Generalization and transfer of contextual cues in motor learning. *J. Neurophysiol.* **2015**, *114*, 1565–1576. [CrossRef]

44. Shadmehr, R.; Mussa-Ivaldi, F.A. Adaptive representation of dynamics during learning of a motor task. *J. Neurosci.* **1994**, *14*, 3208–3224. [CrossRef]

45. Thoroughman, K.A.; Shadmehr, R. Learning of action through adaptive combination of motor primitives. *Nature* **2000**, *407*, 742–747. [CrossRef]